RESEARCH PAPER
https://doi.org/10.1071/WF24161

International Journal of WILDLAND FIRE
International Association of Wildland Fire

# Assessing wildland fire suppression effectiveness with infrared imaging on experimental fires

Melanie Wheatley[A,*,§], Joshua M. Johnston[B], B. Mike Wotton[A,B], Douglas G. Woolford[C] and David L. Martell[A]

For full list of author affiliations and declarations see end of paper

***Correspondence to:**
Melanie Wheatley
Institute of Forestry and Conservation, John H. Daniels Faculty of Architecture, Landscape and Design, University of Toronto, Toronto, ON M5S 3B3, Canada
Email: melanie.wheatley@ontario.ca

[§]This research was carried out while MW was a PhD student at the University of Toronto. MW is currently employed with the Ministry of Natural Resources, Aviation Forest Fire Emergency Services and all correspondence should be directed to melanie.wheatley@ontario.ca.

**Received:** 25 September 2024
**Accepted:** 7 January 2025
**Published:** 23 January 2025

**Cite this:** Wheatley M *et al.* (2025) Assessing wildland fire suppression effectiveness with infrared imaging on experimental fires. *International Journal of Wildland Fire* **34**, WF24161. doi:10.1071/WF24161



## ABSTRACT

**Background.** Suppression effectiveness is often evaluated by measuring the extent to which it slows fire spread and reduces fireline intensity. Although studies have used infrared (IR) imaging methods to explore suppression effectiveness, most do not measure or assess the influence of water application on energy release. **Aims.** This preliminary analysis uses IR imagery to quantify the impact of suppression on fire behaviour and the reduction in energy released from a flaming fire. **Methods.** We conducted a series of small-scale experimental burns representative of pine and grass surface litter in the Canadian boreal forest and suppressed these fires while actively monitoring fire behaviour with overhead IR imagery. We used detailed measurements of fire radiative power to estimate fire radiative energy density, forward rate of spread and fireline intensity. **Key results.** We observed changes in fire behaviour due to suppression, quantified the duration of those reductions and detected a suppression signal through an analysis of radiative energy during the flaming combustion phase. **Conclusions.** IR methodology is able to capture the changes in energy released from a fire due to known aspects of water application. **Implications.** Our findings can inform methodologies for field studies on suppression effectiveness, where ground sampling techniques are impractical but airborne IR methods can be employed.

**Keywords:** Byram's fireline intensity, experimental burning, fire management, fire radiative energy density, fire radiative power, fire suppression, infrared imaging, rate of spread, remote sensing, suppression effectiveness, wildfire.

## Introduction

In Canada, an average of nearly 3 million ha of forest is burned by wildland fires every year (Canadian Interagency Forest Fire Centre (CIFFC) 2021), with almost CA$1 billion spent annually on wildland fire management (Stocks and Martell 2016). Although fires are a natural disturbance and they can provide ecological benefits, wildland fire management agencies commonly suppress fires to mitigate the potentially disastrous social and economic impacts of wildland fires.

Initial attack ground suppression crews are personnel that are trained, equipped and deployed to conduct initial suppression action on fires to halt fire spread (Merrill and Alexander 1987; CIFFC 2023). The suppression tactics and equipment initial attack crews use to build fire line in the province of Ontario include hand tools, soft backpack pumps, portable power pumps with hose and heavy machinery (e.g. dozers). Ground suppression can include the use of both direct and indirect suppression tactics. Where water is available, direct suppression by ground crews often consists of 'knocking down flames', adding water to the combustion zone to decrease the rate at which energy is released by the fire (and thereby slow its growth), and mop-up of residual smouldering or glowing combustion using pumps and hose. In Ontario, indirect suppression is more commonly carried out by airtankers, and consists of wetting the fuels ahead of the fire front, with the aim of slowing fire spread once the fire reaches the treated area.

Suppression effectiveness can be examined at the flame, fireline, incident and landscape scales (Plucinski 2019*a*, 2019*b*). Evaluating fire suppression effectiveness at the

flame or fireline scale often addresses two main factors. First, it estimates the extent to which the suppression action slows the advance of the flame front, essentially, the extent to which it reduces the fire's rate of spread. Second, it focuses on the extent to which suppression decreases fireline intensity, the rate of energy release per unit time per unit length of fire front (in units of kilowatts per metre), which is often described using visual characteristics such as flame length, height and depth (Byram 1959).

One approach to assessing suppression effectiveness at the flame scale is by observing the experimental burning of fuel beds in combustion wind tunnels. This method allows researchers to control factors such as fuel load, moisture content and wind speed. Studies focused on the flame scale have examined both indirect and direct suppression effectiveness (Giménez *et al.* 2004; Àgueda *et al.* 2008; Plucinski 2019*a*). Indirect suppression studies typically focus on suppression enhancers (Gibos and Ault 2007) or retardants (Plucinski and Sullivan 2024) as opposed to water alone. Stechishen (1970) and Stechishen and Little (1971) conducted laboratory experiments using direct suppression methods, and developed equations that related the water depth required to extinguish low-intensity fires (<1000 kW/m) in pine litter fuel beds. Other direct suppression studies using combustion wind tunnels have compared the effectiveness of various gels, foams and retardants (Blakely 1985; Blakely 1990; Plucinski *et al.* 2017; Plucinski and Sullivan 2024) to produce estimates of the suppressant volume per unit area required to extinguish flaming combustion (Plucinski *et al.* 2017; Plucinski and Sullivan 2024).

Emerging innovative technologies based on the use of remote sensing infrared (IR) imagery have been used at incident and fireline scales, to quantify fire behaviour attributes with enhanced spatial and temporal resolution, eliminating the need for ground sampling (e.g. Loane and Gould 1986; George 1985, 1988; Budd *et al.* 1997). Such remote sensing studies have often focused on processing IR data to quantify aerial suppression drop effectiveness. Suppression effectiveness has been measured using a 'cooling factor' by comparing the temperature of the drop zone before and after suppression (e.g. Pérez *et al.* 2011), and changes in fire spread rate, measured by analysing the percentage reduction of the short-term (i.e. 1 min) rate of spread in the drop area (e.g. Plucinski and Pastor 2013).

An important missing component of these experiments is the ability to objectively quantify the influence of suppression on energy released from the combustion zone, which is essentially the change in fireline intensity due to that suppression action. Physics-based models, which predict the theoretical water amounts required to extinguish fires of various fireline intensities, are often used as surrogate measures to fill this gap in our understanding of the impact of suppression on the combustion process (e.g. Hansen 2012; Penney *et al.* 2019; Van Wagner and Taylor 2022). The increasing availability of remote sensing technologies to fire management agencies (e.g. Johnston *et al.* 2020; McFayden *et al.* 2023*a*) offers opportunities to assess the extent to which such technology can be used to study the direct impacts of suppression on a fire front.

Previous studies have established methods for estimating both forward rate of spread (e.g. Pastor *et al.* 2006; Paugam *et al.* 2012; Johnston *et al.* 2018) and Byram's fireline intensity (e.g. Johnston *et al.* 2017) using IR imagery of experimental fires. Byram's fireline intensity, in kilowatts per metre, is commonly represented by the following equation:

$$I_B = H \times w \times r$$

where $H$ is the heat of combustion (kJ/kg), $w$ is the mass of the available fuel per unit area (kg/m$^2$) and $r$ is the rate of spread (m/s). An alternative formulation proposed by Byram (1959) that can be used to calculate frontal fireline intensity when measuring inputs using IR methods is:

$$I_B = E_{tot} \times r$$

where $E_{tot}$ represents the total available fuel energy per unit area (kJ/m$^2$). $E_{tot}$ can be estimated using the measured Fire Radiative Power (FRP) or Fire Radiative Power Density (FRPD) when accounting for pixel area. The temporal integration of FRP produces Fire Radiative Energy, or Fire Radiative Energy Density (FRED), representing the total radiative energy released from the fire during combustion. FRED can therefore be used to estimate the total fuel consumed (Wooster *et al.* 2003, 2005), and hence $E_{tot}$, but requires scaling by an estimate of the radiative fraction to yield the total energy release (Johnston *et al.* 2017).

The need for further suppression effectiveness research was discussed nearly three decades ago (Hirsch and Martell 1996), but since then, there has been little scientific research to explore this problem (Plucinski 2019*a*, 2019*b*). Although some authors have demonstrated that remote sensing technology can be used to measure the spatial and temporal variation in fire behaviour metrics (e.g. Johnston *et al.* 2017, 2018), there have been few studies that have aimed to quantify suppression effectiveness using such technology. As emerging technology and remote sensing capabilities will be increasingly available to provide near real-time information to support fire management operations and response decision-making (e.g. WildFireSat; Johnston *et al.* 2020; McFayden *et al.* 2023*a*), an improved understanding of suppression effectiveness on spreading wildfires could be enhanced by these newly available data.

In this study, we conduct a preliminary exploration of how water delivered during ground suppression operations influenced the behaviour of a series of small experimental fires representative of the boreal forest using measurements of fire intensity and rate of spread obtained from IR

imagery. For the period immediately before and after suppression, we explicitly examine the influence of two different water application approaches and two different water volumes on:

1. Fire behaviour expressed in terms of the immediate change in both fireline intensity and rate of spread;
2. The duration of holding time for the observed suppression-induced reduction in fire behaviour (i.e. the time required for a fire to resume spreading actively after suppression);
3. The energy released from a fire, as measured by a decrease in FRED.

The first two measurements described above can be used to estimate the influence of suppression on flame front advance and holding time. The third allows us to explore whether the direct energy sink of water applied to a combustion zone as part of ground suppression can be measured by IR imaging.

## Methods

Experimental burns were conducted to observe the impact of fire suppression (i.e. the depth of water applied on and in advance of a flaming fire front) on fire behaviour. Several treatment factors were investigated including fuel type, fuel load, suppression type and the amount of water applied. IR imaging cameras mounted on a 30-m scaffold tower beside the experimental burn plots were used to measure both fire intensity and rate of spread throughout the duration of each burn.

### Data collection

#### Experiment description

Twenty-two experimental burns were conducted between 5 and 12 September 2019 at the Canadian Forest Service's Rose Experimental Burn Station, near Thessalon, Ontario, Canada. A burn platform of 7.34 × 4.88 m was located at the base of a 30-m scaffold tower where IR imagery cameras and one visual camera were mounted 15 m above the platform and angled (~21°) to capture the full platform within their field of view (see Table 1 for IR camera specifications). The base of the burn platform consisted of 12 'fire-proof' Marinite boards arranged into three rows of four panels (2.34 × 1.21 m). This experimental burn set-up and IR imagery methodology for measuring fire behaviour has been used in previous studies at this location (e.g. Johnston *et al.* 2017, 2018). Fig. 1 is an annotated photograph of the burn platform and tower.

#### Fuel types and arrangement

Prior to the burns, a bed of cured fine fuels was evenly distributed on each panel of the burn platform. Two different fine fuel types were used: dried longleaf pine needles (*Pinus palustris*), and cut and cured Timothy grass (*Phleum pretense*). Although stored in a location that was mostly sheltered from rainfall, storage was not environmentally controlled and moisture content in both fuel types varied with ambient conditions on the day of the burn.

All fuel was sorted and dispersed to remove coarse woody material to ensure the fuel consisted of only fine fuels. Two different fuel loadings were used: a moderate fuel loading consisting of a wet mass of 1.0 kg/m$^2$ of fuel and a heavy fuel loading consisting of a wet mass of 1.5 kg/m$^2$ of fuel. The moderate fuel load of 1.0 kg/m$^2$ of pine needles has been used in previous experiments at this site (e.g. Johnston *et al.* 2017, 2018) and sustainably carried spreading fires through the entire fuel bed. The heavy fuel load was chosen to represent 50% more fuel, to potentially generate higher-intensity fires. All of the 12 sections of the fuel bed (Fig. 1) were loaded with the same amount of fuel to ensure homogeneity in the distribution of the fuel across the burn pad. Ten fuel bed moisture samples (~20–30 g per sample; this sample weight is ~1% of the fuel on each panel in the moderate fuel load grouping and it is therefore reasonable to assume that it did not impact the fire intensity calculation while still providing a robust moisture sample) were taken 5 min prior to each burn, one from each of the outer sections of the fuel bed (all sections excluding nos 6 and 7 in Fig. 1). Samples were weighed and dried in the lab at 95°C for 24 h and an average moisture content (gravimetric moisture by dry weight) for each fuel bed was calculated. Fuel bed depth was also measured on the outer sections of the fuel bed prior to the burn and used to calculate an overall average depth and fuel bed bulk density.

**Table 1.** Specifications of the mid-wave infrared (MWIR) and long-wave infrared (LWIR) cameras used in the experiment.

| Data | MWIR | LWIR |
|---|---|---|
| Infrared imagery | FLIR SC6703 | FLIR T450SC |
| Detector array | 640 × 512 | 320 × 240 |
| Spectral band | Narrow 3.9 μm filter | 8–14 μm |
| Dynamic range (K) | 423–1123 | 273–1773 |
| Imaging approach | Superframing three integration times | Single integration time |
| Frame rate (Hz) | 45 | 30 |

#### Suppression treatments

The experimental suppression treatment applied to each fire was water delivered from soft backpack pumps with a jet stream nozzle. Two different water application tactics were used: direct and indirect suppression. During direct suppression, water was precisely targeted using a forceful stream directly into the flaming combustion zone of the fire

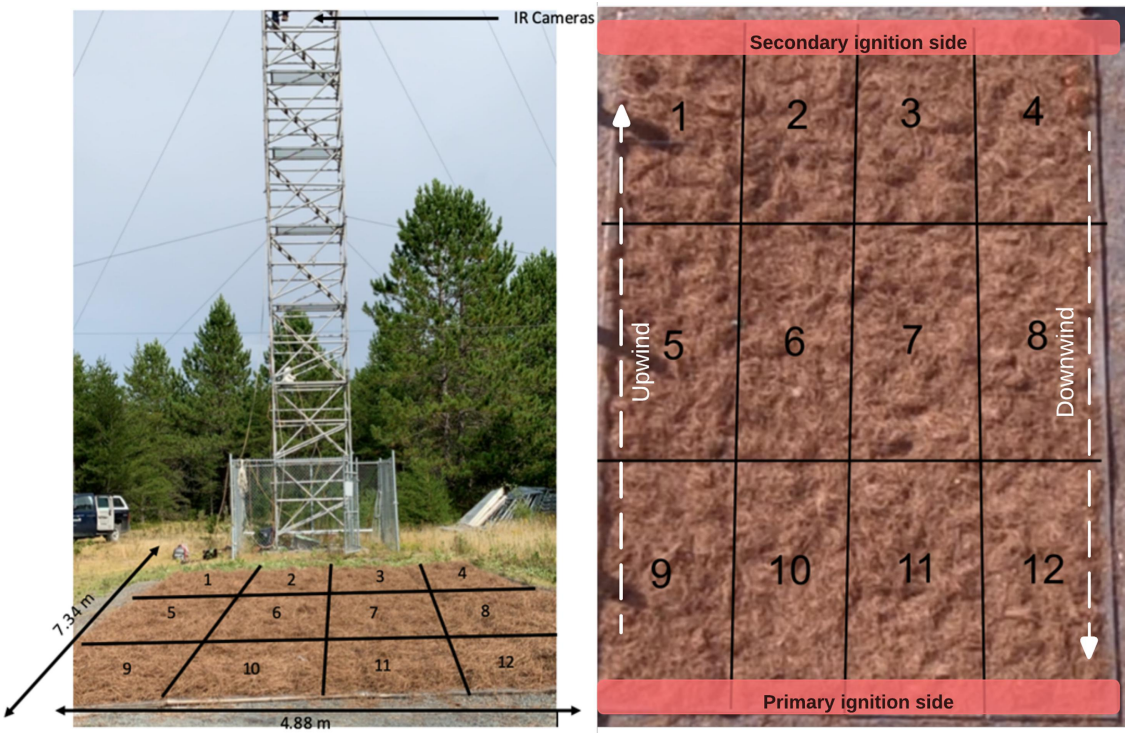


**Fig. 1.** Annotated photograph of the experimental burn platform. The fuel bed is 7.34 by 4.88 m and comprises 12 Marinite boards. Fuel moisture samples were taken from each outside edge panel (i.e. all panels excluding panels 6 and 7) and fuel consumption measurements (i.e. post-fire ash weight) were taken for each panel immediately after the burn. Primary ignition occurred (when the general wind direction was upwind from the platform) on panels 9–12, whereas secondary ignition (when the general wind direction was downwind from the platform) occurred on panels 1–4.

front. For indirect suppression, water was applied with a dispersed stream on the fuel immediately ahead of the advancing fire front and sprayed to attempt to cover a wider coverage area, targeting a suppression width of 30 cm. Although typically ground suppression in Ontario does not involve indirect suppression using backpack pumps, this wetting of the fuels ahead of the flame front is sometimes used by aerial suppression and in sprinkler applications. Indirect suppression provided an opportunity to mimic the wetting of fuels of aerial suppression while also providing paired contrasts with direct combustion zone suppression.

There were two different dose levels for suppression: a low suppression effort amount consisting of '10 pumps' or approximately 1000 mL of water delivered in total, and a high suppression effort amount consisting of '16 pumps' or approximately 1600 mL of water. Water amounts were delivered uniformly across the width of the fuel bed.

### Experiment execution

We ignited each burn using a standard forestry drip torch across the width of the fuel bed along the upwind side of the platform (typically panels 9–12 in Fig. 1). When wind flow was in the opposite direction, the ignition line spanned panels 1–4 to ensure the fire was spreading with the wind and exhibiting head fire spread; this occurred for six of the burns (B15, B16, B17, B18, B19, B21 in Table 2). Two suppression treatment passes were made during each burn. The first suppression pass was delivered once the flame front had spread a third of the distance down the burn pad (2.34 m). The fire was left to re-establish and to then spread another third down the burn pad before the second suppression pass. The suppression tactic used for the first and second suppression passes alternated between indirect and direct suppression (i.e. if the first suppression pass for a burn was direct suppression, then the first suppression pass for the next burn would be indirect suppression), with each suppression tactic being used once for each burn. The suppression dose level (i.e. low and high water) was held constant for the two suppression passes on a specific burn but varied between the two dose levels from burn to burn. Note that in some cases, suppression eliminated the re-establishment of sustainable flaming spread and the fire had to be re-ignited (the decision to re-ignite was made if the fire was exhibiting no flaming or active spread after 5 min since the suppression treatment and it was clear that glowing combustion was decreasing, and the fire was approaching extinguishment). In these cases, the establishment of fire spread was consistent with the first observation

**Table 2.** Pre-burn information for each of the 22 experimental burns.

| Burn ID | Date/time (dd/mm/year, hours) | Fuel type | Fuel load (kg/m$^2$) | Average fuel depth (s.e.) (cm) | Amount of water applied | Average moisture content (s.e.) (%) | Weather | | | |
|---|---|---|---|---|---|---|---|---|---|---|
| | | | | | | | Temperature (°C) | Relative humidity (%) | Wind speed (km/h) | Maximum wind speed (km/h) |
| B1 | 05/09/2019 18:30 | Pine | 1.0 | 8.1 (0.3) | High | 22.4 (1.99) | 21.9 | 47 | 7.6 | 16.3 |
| B2 | 08/09/2019 10:24 | Pine | 1.0 | 9.1 (0.4) | Low | 24.8 (1.04) | 3.3 | 97 | 1.1 | 5.9 |
| B3 | 08/09/2019 11:33 | Pine | 1.0 | 7.4 (0.3) | High | 25.3 (1.39) | 3.6 | 97 | 4.1 | 9.1 |
| B4 | 08/09/2019 13:17 | Pine | 1.5 | 11.9 (0.5) | Low | 21.7 (1.49) | 7.8 | 97 | 5.9 | 13.1 |
| B5 | 08/09/2019 14:26 | Pine | 1.5 | 12.2 (0.4) | High | 22.7 (1.23) | 14.2 | 53 | 5.1 | 15 |
| B6 | 08/09/2019 16:00 | Pine | 1.0 | 7.1 (0.4) | Low | 25.0 (2.06) | 14 | 50 | 6.4 | 15.5 |
| B7 | 09/09/2019 12:55 | Pine | 1.0 | 7.3 (0.3) | High | 21.6 (1.54) | 2 | 95 | 0.6 | 2.1 |
| B8 | 09/09/2019 14:00 | Pine | 1.5 | 10.3 (0.5) | Low | 17.4 (1.05) | 11.6 | 96 | 2.6 | 7.4 |
| B9 | 09/09/2019 15:14 | Pine | 1.0 | 6.8 (0.3) | Low | 36.0 (5.02) | 16.5 | 55 | 5.2 | 11.6 |
| B10 | 09/09/2019 16:14 | Pine | 1.0 | 7.3 (0.3) | High | 25.4 (2.33) | 16.4 | 53 | 6 | 14.5 |
| B11 | 09/09/2019 17:08 | Pine | 1.0 | 7.4 (0.3) | Low | 26.2 (2.77) | 16.3 | 50 | 4 | 17.8 |
| B12 | 11/09/2019 11:57 | Grass | 1.0 | 16 (0.4) | Low | 14.7 (0.41) | 13.5 | 94 | 3.4 | 17.4 |
| B13 | 11/09/2019 13:15 | Grass | 1.0 | 19.8 (0.8) | High | 13.0 (0.34) | 13.7 | 88 | 5.5 | 12.8 |
| B14 | 11/09/2019 14:12 | Grass | 1.0 | 17.9 (0.7) | Low | 9.9 (0.35) | 13.8 | 84 | 8 | 17.9 |
| B15 | 11/09/2019 14:50 | Grass | 1.0 | 15.9 (0.5) | High | 12.7 (0.36) | 14.8 | 77 | 4.9 | 16.1 |

(*Continued on next page*)

**Table 2.** (*Continued*)

| Burn ID | Date/time (dd/mm/year, hours) | Fuel type | Fuel load (kg/m$^2$) | Average fuel depth (s.e.) (cm) | Amount of water applied | Average moisture content (s.e.) (%) | Weather | | | |
|---|---|---|---|---|---|---|---|---|---|---|
| | | | | | | | Temperature (°C) | Relative humidity (%) | Wind speed (km/h) | Maximum wind speed (km/h) |
| B16 | 11/09/2019 15:30 | Pine | 1.0 | 4.5 (0.5) | Low | 25.8 (2.21) | 15.4 | 75 | 3.8 | 13.5 |
| B17 | 12/09/2019 11:55 | Grass | 1.0 | 13.7 (0.5) | Low | 11.1 (0.53) | 7.1 | 90 | 2.7 | 10.5 |
| B18 | 12/09/2019 12:38 | Grass | 1.0 | 16.5 (0.3) | High | 9.2 (0.21) | 9.9 | 76 | 7.3 | 17.4 |
| B19 | 12/09/2019 13:50 | Grass | 1.0 | 15 (0.5) | Low | 7.0 (0.17) | 12.5 | 65 | 9.4 | 27.4 |
| B20 | 12/09/2019 14:35 | Grass | 1.0 | 13.9 (1.2) | High | 6.6 (0.19) | 14.4 | 59 | 7.8 | 21.3 |
| B21 | 12/09/2019 15:40 | Grass | 1.0 | 14.6 (0.7) | Low | 9.5 (0.66) | 16.2 | 52 | 8.8 | 20.8 |
| B22 | 12/09/2019 16:30 | Grass | 1.0 | 12.4 (0.4) | High | 9.9 (0.79) | 17.2 | 51 | 7.4 | 20.3 |

The weather observations are from the closest hour to when the fire was ignited. Maximum wind speed reflects the maximum wind speed within the hour the fire was ignited. s.e., standard error.

before the second suppression pass occurred. Once each burn was complete, the residual ash was collected immediately and weighed by burn panel to provide a measure of the fuel consumption. Note that the application of water required individuals to walk across the burn pad, which may have compacted fuels; however; we feel that the variability in wind and its subsequent effect on fire behaviour would have masked the effects of any small, compressed pockets of fuel on the burn pad. Table 2 shows details for each experimental burn, including fuel type, fuel load, fuel depth, suppression amount, moisture content of fuels and weather. Weather observations (i.e. temperature, relative humidity, wind speed and maximum wind speed) were recorded by a fixed station located 100 m from the burn site with an anemometer height of 10 m. The weather observations collected are from the closest hour to when the fire was ignited.

Each burn was observed using two IR cameras, one mid-wave infrared (MWIR) and one long-wave infrared (LWIR) and a visual imagery video camera, all mounted 15 m above the platform. The MWIR camera was used to capture spatial and temporally detailed thermal imagery used to estimate fire intensity and rate of spread, which allowed us to estimate the change in fire behaviour as a result of suppression actions. The methods used are consistent with those described in Johnston *et al.* (2017, 2018). The LWIR camera was used for ambient thermal imaging and to capture the timing and coverage area of water application. The visual imagery was used to reference fire behaviour attributes from the IR camera.

### Data processing

The IR imagery was extracted at 2 Hz for both the MWIR and the LWIR imagery. For data processing of fire behaviour measurements, the MWIR data were orthorectified (i.e. removing image distortions due to the camera angle) using the burn pad features for reference. A direct linear transformation was applied to reproject the pixel radiance data into a uniform 10-cm grid while conserving energy, creating a constant pixel size across the full burn extent (e.g. Paugam *et al.* 2012; Johnston *et al.* 2017, 2018). The corrected 10-cm resolution IR data were processed to produce estimates of five different fire behaviour attributes: rate of spread (m/min) (Fig. 2*b*), FRP (kW), FRPD (kW/m$^2$), FRED (kJ/m$^2$) (Fig. 2*c*) and fireline intensity (kW/m) (Fig. 2*d*) (Table 3). Supplementary Appendix S1 summarises the data processing procedures applied to each of these outputs.

### Overview of data analysis

In the analysis of the effect of suppression on fire behaviour and fireline holding time, the spatial IR data for each burn were extracted to isolate the inner two rows (2.44 m; rows 2 and row3), or panels 2, 3, 6, 7, 10 and 11 of the burn platform (Fig. 3) to eliminate potential edge effects. The first 1 m strip of pixels on the end of the platform where ignition occurred was omitted from the analysis to remove surges in fire behaviour during ignition (Fig. 3). Note that in analyses reported here, row 2 and row 3 are treated as separate experimental units. Therefore, for each of the 22 experimental burns, there are two observations of fire behaviour summarised from the pixel-based information derived from the IR imagery (one for row 2 and one for row 3; each row is 1.22 m wide) to produce 44 different experimental observations. For each row, time series of rate of spread and fireline intensity were created for each of these burns to show changes in fire behaviour based on the fire arrival time at each pixel (Table 3). To obtain a more robust estimate of temporal fluctuations in fire behaviour, the pixel observations (for each row) were grouped for each second, and the median fire behaviour observation for each second in the data was used.

## Analysis and results

The summary of fire behaviour metrics for each of the experimental burns is listed in Table 4. The average pre-suppression rate of spread was 0.61 m/min for pine fuels and 1.40 m/min for grass fuels. The average fireline intensity was 118 kW/m for pine fuels and 245 kW/m for grass fuels, which corresponds to the mid-range of fire intensity Class 2 as defined by the Field Guide to the Canadian Fire Behaviour Prediction (FBP) System (Taylor and Alexander 2018). The following sections provide the results of the analysis of our experimental observations arranged by the three distinct measurements outlined in the Introduction.

### Impact of suppression on fire behaviour

#### Objective

This analysis was designed to examine the impact of fire suppression treatments on both rate of spread and fireline intensity by using time series data for each row of the burn pad and examining the period immediately before and after suppression.

#### Analysis

Pre-suppression fire behaviour estimates were obtained using the 10-s interval prior to the time when suppression began, and post-suppression fire behaviour estimates were obtained using the 10-s interval after the application of suppression. For direct suppression, pre-suppression estimates were calculated using the median observations during the 10-s interval prior to the time suppression began, and post-suppression estimates were calculated using observations during the 10-s interval after the application of

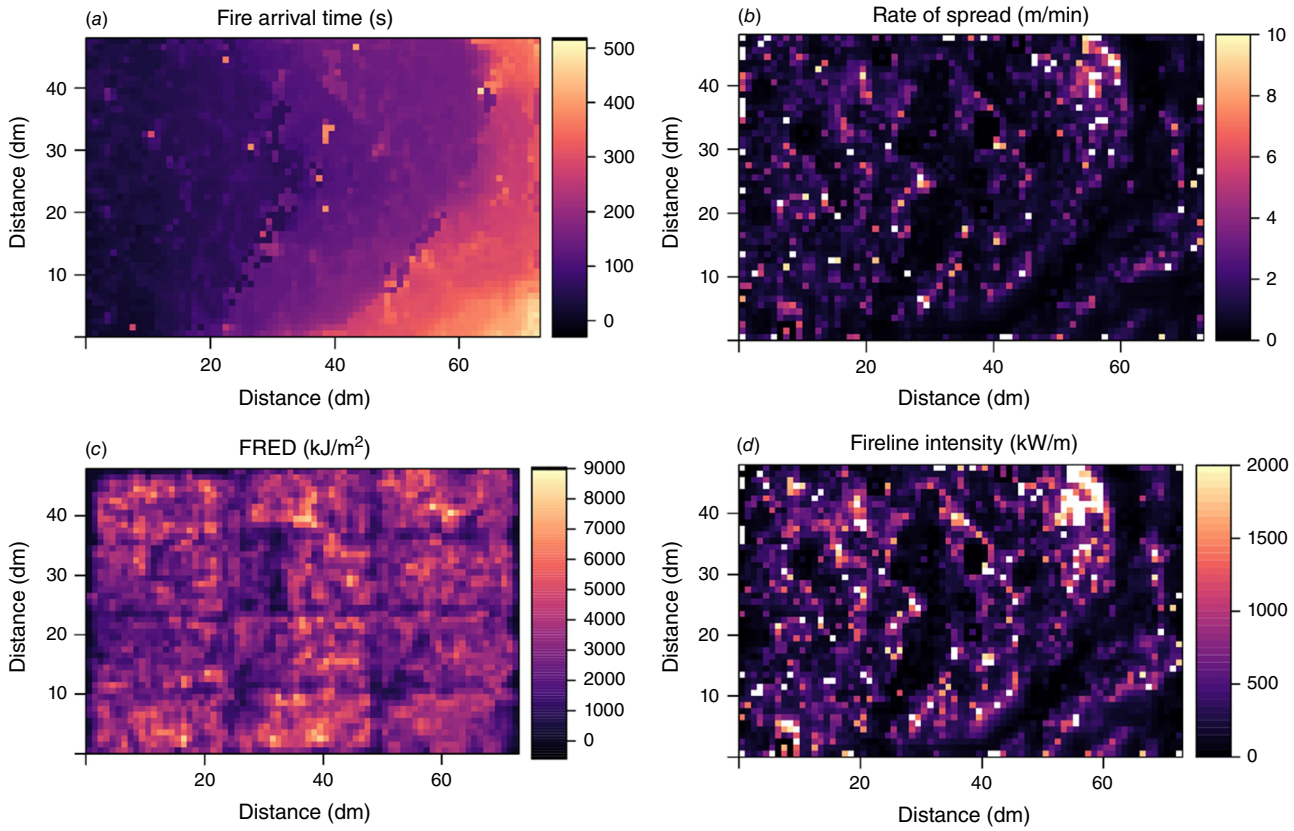


**Fig. 2.** Images of four fire behaviour attributes measured for a single burn (B8). Burn pad is rotated 90° clockwise from the layout in Fig. 1. Ignition occurred on the leftmost edge and the fire spread to the right. The *x* and *y* axes represent the distance from the lower left corner in decimetres. (*a*) Fire arrival time in seconds, at each 10 × 10 cm pixel on the burn pad. (*b*) Estimated rate of spread (m/min) at the arrival time in each 10 × 10 cm pixel. (*c*) FRED (kJ/m$^2$) for each 10 ×10 cm pixel. (*d*) Fireline intensity (kW/m) for each 10 × 10 cm pixel. Note that the white pixels in (*b*) and (*d*) represent pixels for which the attributes were beyond the upper thresholds in the axes shown.

suppression across the 1.22 m panel. For indirect suppression, the time suppression took place was not the time when the flame front reached the area where water had been applied, as the water was applied slightly ahead of the flame front. We used the LWIR imagery to estimate the time the flame front reached the treated area and the time when the flame front passed beyond the treated area. Therefore, the pre-suppression time interval ended when the flame front reached the start of the treated area and began 10 s prior to that point. The 10-s post-suppression time interval started after the entire flame front had reached the treated area. In some cases, after suppression was applied, the fire moved so slowly that it stayed within the same pixel for the entire 10-s duration. To estimate rate of spread for these missing time periods when the fire exhibited no active spread, we used the next observation of fire spread.

To calculate a 'fire behaviour difference' value, the median post-suppression value was subtracted from the median pre-suppression value for both the rate of spread (referred to as $ROS_{diff}$) and fireline intensity (referred to as $FI_{diff}$). This method of estimating $ROS_{diff}$ and $FI_{diff}$ was repeated for rows 2 and 3 in each of the burns (i.e. 44 $ROS_{diff}$ values and 44 $FI_{diff}$ values).

To quantify the impact of the four treatments on fire behaviour, two different four-way factorial ANOVA comparisons were made, one using $ROS_{diff}$ as the metric of comparison and the other using $FI_{diff}$ for each burn. When treatment groups or interactions between treatments showed strong evidence of a difference between groups ($P < 0.05$), Tukey's Honest Significant Difference post-hoc tests were used to determine which specific treatment group means were different and to identify the direction of any such differences.

The influence of the pre-suppression fire behaviour on the difference in fire behaviour was also examined in terms of the extent to which this relationship varied with suppression type and the amount of water applied. After graphical exploration of these data, two different linear regression models were developed: one for indirect suppression and one for direct suppression. In both models, the independent

**Table 3.** Summary descriptions of the five estimated fire behaviour variables investigated.

| Metric | Definition | Imagery requirements | Resolution | Output format |
|---|---|---|---|---|
| Rate of spread | The speed at which the fire is spreading, representative at the time the fire arrived in the pixel, expressed in metres per minute | Time series | Single value for each pixel for which rate of spread was calculated | Median rate of spread for each second for both row 2 and row 3 |
| Fire radiative power | Radiative power emitted per pixel for each time interval, expressed in watts per pixel | Individual frames | Single value for each pixel, for each frame | Sum over all pixels for each 0.5 s interval |
| Fire radiative energy density | Total radiative energy released from the combustion of the fuels in each pixel, expressed in kilojoules per metre squared | Individual frames | Single value for each pixel, summed over duration of the burn | Single value for each pixel |
| Flaming fire radiative energy density | Flaming radiative energy released from the combustion of the fuels in each pixel, expressed in kilojoules per metre squared | Individual frames | Single value for each pixel, summed for a specified time interval (i.e. 45 s for grass, 60 s for pine) | Single value for each pixel |
| Fireline intensity | Measure of the energy released per second from the entire flame front depth, expressed in kilowatts per metre | Time series | Single value for each pixel for which the fire intensity was computed | Median fireline intensity for each second for both row 2 and row 3 |

Imagery requirements describes the input imagery required to calculate the metric. Resolution represents the spatial and temporal resolution for the processed output. Output format represents the output used for the analysis once the IR data have been manipulated.




**Fig. 3.** (*a*) Layout of the burn pad that depicts each 'row' on the burn platform (Fig. 1*b* rotated 90° clockwise). Most of the experimental fires were ignited along the leftmost edge from top to bottom and spread to the right. Rows 1 and 4 were removed from fire behaviour analysis to eliminate any potential edge effect. The first 1 m strip of pixels where ignition occurred was removed from analysis to remove surges in fire behaviour during ignition. The inner two rows (row 2 and row 3) were treated as separate burns. (*b*) Example of a burn (B9) showing fire behaviour before suppression, and (*c*) immediately after indirect suppression was applied.

variables were the 10-s average pre-suppression fire behaviour estimate, the amount of water applied (i.e. low or high) and an interaction term between the two, with the response variable being either $ROS_{diff}$ or $FI_{diff}$.

**Table 4.** Summary of fire behaviour attributes measured or estimated for each experimental burn.

| Burn ID | Fuel type and dry fuel load (kg/m$^2$) | Dry fuel consumption (kg/m$^2$) | Rate of spread (m/min) | Fireline intensity (kW/m) | FRED (kJ/m$^2$) | F-FRED (kJ/m$^2$) |
|---|---|---|---|---|---|---|
| B1 | Pine (0.82) | 0.69 (0.06) | 0.33 (0.08) | 39 (11) | 2247 (1042) | 995 (444) |
| B2 | Pine (0.80) | 0.66 (0.04) | 1.03 (0.21) | 137 (51) | 1718 (1078) | 840 (451) |
| B3 | Pine (0.80) | 0.59 (0.06) | 0.33 (0.12) | 72 (26) | 1490 (808) | 756 (397) |
| B4 | Pine (1.23) | 1.05 (0.07) | 0.55 (0.11) | 165 (60) | 2856 (1609) | 1014 (578) |
| B5 | Pine (1.22) | 1.07 (0.05) | 0.15 (0.07) | 44 (4) | 3085 (1698) | 1019 (546) |
| B6 | Pine (0.80) | 0.66 (0.05) | 0.63 (0.23) | 106 (57) | 1689 (948) | 829 (374) |
| B7 | Pine (0.82) | 0.70 (0.03) | 0.17 (0.05) | 18 (5) | 1436 (739) | 832 (334) |
| B8 | Pine (1.28) | 1.05 (0.07) | 0.77 (0.12) | 233 (56) | 3046 (1339) | 1068 (554) |
| B9 | Pine (0.74) | 0.64 (0.08) | 1.05 (0.46) | 195 (134) | 1877 (911) | 895 (463) |
| B10 | Pine (0.80) | 0.69 (0.04) | 1.41 (0.16) | 258 (32) | 1887 (970) | 903 (501) |
| B11 | Pine (0.79) | 0.68 (0.06) | 0.75 (0.36) | 118 (54) | 1847 (939) | 854 (471) |
| B12 | Grass (0.87) | 0.68 (0.07) | 0.47 (0.01) | 65 (13) | 1487 (800) | 830 (369) |
| B13 | Grass (0.88) | 0.72 (0.07) | 1.92 (0.17) | 352 (13) | 1664 (1002) | 925 (390) |
| B14 | Grass (0.91) | 0.79 (0.03) | 0.47 (0.05) | 44 (10) | 1818 (1068) | 1163 (495) |
| B15 | Grass (0.89) | 0.73 (0.05) | 2.26 (0.18) | 325 (122) | 1637 (1009) | 699 (520) |
| B16 | Pine (0.79) | 0.49 (0.17) | 0.21 (0.06) | 29 (22) | 1252 (676) | 588 (327) |
| B17 | Grass (0.90) | 0.79 (0.03) | 1.04 (0.12) | 133 (93) | 1679 (1003) | 711 (494) |
| B18 | Grass (0.92) | 0.80 (0.03) | 2.50 (0.37) | 454 (101) | 1779 (1030) | 681 (522) |
| B19 | Grass (0.93) | 0.82 (0.03) | 1.88 (0.64) | 483 (229) | 1795 (1020) | 774 (505) |
| B20 | Grass (0.94) | 0.79 (0.07) | 0.87 (0.11) | 167 (4) | 1810 (1065) | 795 (505) |
| B21 | Grass (0.91) | 0.82 (0.04) | 1.18 (0.12) | 224 (35) | 1806 (1137) | 961 (480) |
| B22 | Grass (0.91) | 0.76 (0.08) | 1.35 (0.03) | 198 (62) | 1588 (1090) | 871 (446) |

Mean with s.d. in parenthesis. Fuel consumption represents the average dry fuel consumption across all 12 panels of the burn pad. Rate of spread and fireline intensity represent the mean for rows 2 and 3 for the 10 s before the first water treatment was applied to the fire to avoid bias from both the suppression areas and the associated recovery of spread. Fire radiative energy density (FRED) and flaming fire radiative energy density (F-FRED) are shown for the no-suppression areas of the burn pad.

## Findings

On average, suppression reduced the rate of spread by 0.5 m/min (s.d.  0.7), or ~60%, and fireline intensity by 50 kW/m (s.d.  159), or 50%. For pre- and post-suppression rate of spread and fireline intensity observations, refer to Supplementary Appendix S2. As fireline intensity is a product of estimated rate of spread and FRED, there is a very strong correlation between rate of spread and fireline intensity. We therefore present only the results for the $ROS_{diff}$ analysis here (for $FI_{diff}$ results, see Supplementary Appendix S3).

The four-way ANOVA comparison of $ROS_{diff}$ showed no evidence of differences in fire behaviour across treatment groups except for fuel type, where only weak evidence was observed ($F = 7.00$, $P = 0.1$). Tukey's post hoc test results suggest that for the main effect of fuel type, grass fuels generally exhibited a greater change in fire behaviour than pine fuels ($P = 0.16$). These results are consistent with Fig. 4, showing that the average $ROS_{diff}$ for grass fuels is higher than for pine fuels, a finding likely due to the fact that grass fuels generally supported faster spread rates (Table 4), and therefore had more potential for ROS to decrease. Similarly to the $ROS_{diff}$ findings, the four-way ANOVA comparison showed no evidence of differences in $FI_{diff}$ across treatment groups except for fuel type ($F = 5.2$, $P = 0.03$).

The analysis of the relationship between the pre-suppression rate of spread and the average $ROS_{diff}$ showed a positive linear relationship between the two variables (Fig. 5), with strong evidence ($P < 0.001$) of this increasing relationship for both indirect and direct suppression (Table 5). For fires with greater spread rates, the $ROS_{diff}$ is greater than fires with slower spread rates, which would imply that both treatments are reducing spread rate to the minimum level that is measurable with the IR camera and arrival time methodology we used. However, this

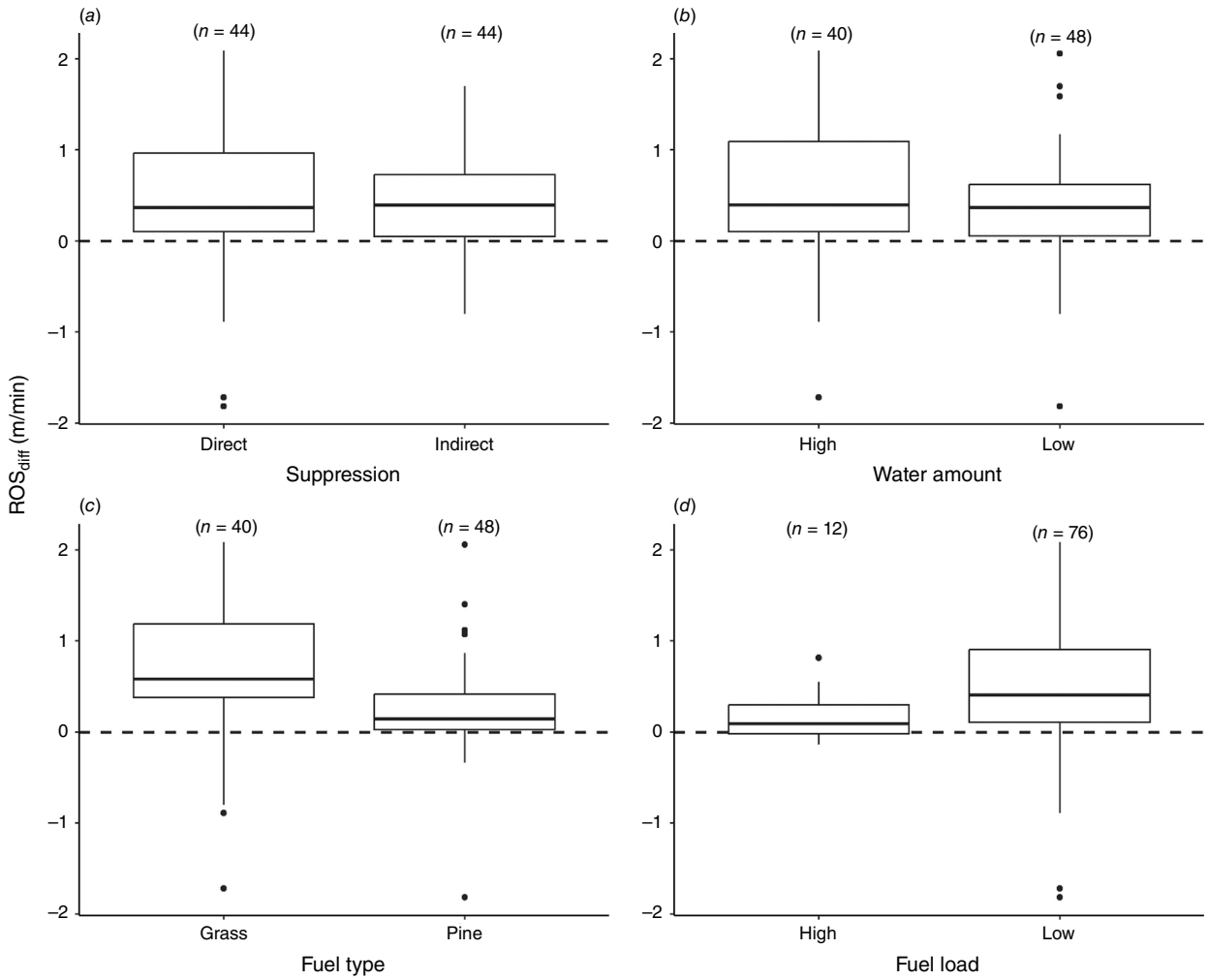


**Fig. 4.** Boxplots of the difference in spread rate before and after suppression, $ROS_{diff}$ ($y$-axis; units are metres per minute), for each of the four treatment groups examined: (*a*) suppression; (*b*) water amount; (*c*) fuel type; (*d*) fuel load. The grey dashed line ($y$ = 0 m/min) indicates no change is observed pre and post suppression treatment. In some cases, the post-suppression rate of spread was higher than the pre-suppression rate of spread (as indicated by a negative $ROS_{diff}$).

relationship does not seem to change between indirect and direct suppression, and there seems to be little influence of the amount of water applied on $ROS_{diff}$ (as indicated by the absence of evidence of an interaction between water amount and pre-suppression rate of spread in Table 5).

As the area treated varied between the two suppression techniques, the amount of water per unit area (as determined using estimates of coverage area from the LWIR imagery) applied to the fuel differed; the depth of water delivered was equivalent to approximately 1.4 and 2.3 mm for the low and high water direct suppression treatments respectively, and 0.7 and 1.1 mm for the low and high water treatments for indirect suppression. In these experiments, we applied more water than the amount suggested in fire suppression models to extinguish fires with a flame front fire intensity of 1000 kW/m (e.g. Loane and Gould (1986) and McFayden *et al.* (2023*b*) suggest ~0.5 mm of water is required to extinguish a flame front with a fire intensity of 1000 kW/m for pine fuels). Although the water depths applied did reduce spread rate to nearly zero, the fires often continued to burn and were not completely extinguished. The discrepancy between our results and those from the literature may stem from differences in how water was applied, as models (e.g. Loane and Gould 1986, McFayden *et al.* 2023*b*) usually assume water is uniformly distributed across the entire combustion zone, reducing the energy levels in all portions of the combustion zone and eliminating potential reheating to ignition temperatures. In our experiment, water was applied to the actively flaming portion of the combustion zone at the leading edge of the flame front and, as a result, the glowing combustion of the litter bed remained active. The partially consumed fuel in these areas continued to release energy, reheating the unburned fuels nearby.

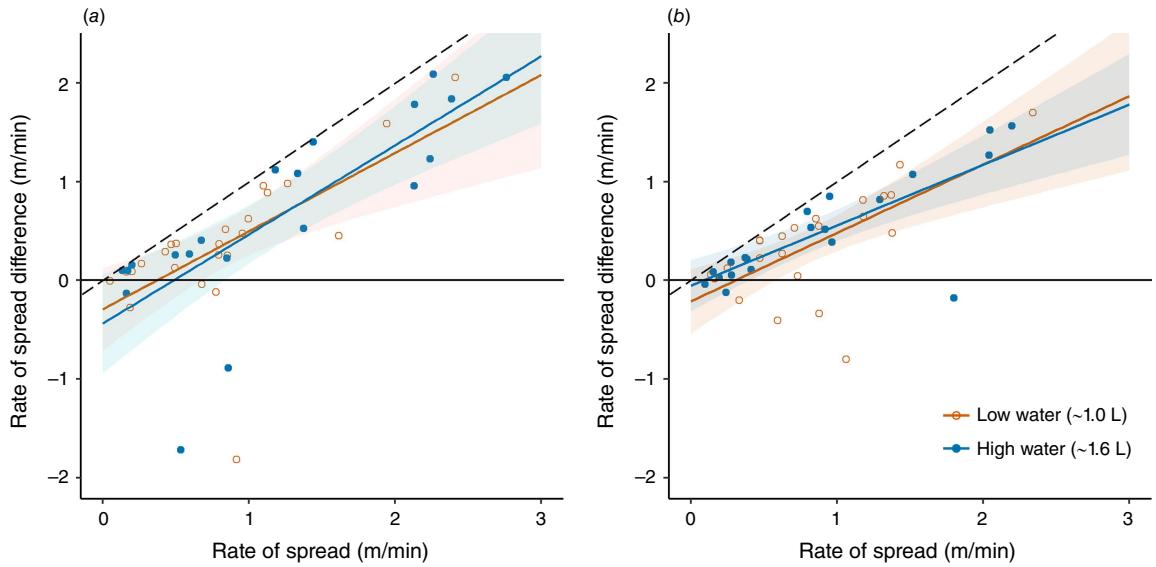


**Fig. 5.** Observations and regression lines of the average rate of spread before suppression compared with the average $ROS_{diff}$ for both (*a*) direct, and (*b*) indirect suppression. This figure shows four regressions: one for low and high water for each suppression type. The solid horizontal black line at $y = 0$ represents the theoretical relationship that we would see if suppression did not have any influence on fire behaviour (i.e. $ROS_{diff} = 0$). The dashed $y = x$ line represents the theoretical relationship that we would see if suppression always reduced rate of spread to 0, indicating that any amount of water applied was fully effective at eliminating spread. Models were built using the following number of observations: direct suppression, low water ($n = 24$); direct suppression, high water ($n = 20$); indirect suppression, low water ($n = 24$); indirect suppression, high water ($n = 20$).

**Table 5.** Regression analysis comparing the pre-suppression average rate of spread and the $ROS_{diff}$.

| | | Coefficient (s.e.) | | *P*-value |
|---|---|---|---|---|
| Direct | Intercept | −0.44 | (0.23) | 0.06 |
| | Pre-suppression ROS | 0.90 | (0.16) | <0.001 |
| | Water (Low = 1) | 0.14 | (0.31) | 0.65 |
| | Pre-suppression ROS × Water | −0.11 | (0.26) | 0.68 |
| Indirect | Intercept | −0.05 | (0.14) | 0.70 |
| | Pre-suppression ROS | 0.61 | (0.12) | <0.001 |
| | Water (Low = 1) | −0.16 | (0.20) | 0.43 |
| | Pre-suppression ROS × Water | 0.08 | (0.19) | 0.68 |

Two generalised linear regression models were fit, one for direct suppression ($n = 44$) and one for indirect suppression ($n = 44$). Interaction terms between pre-suppression rate of spread (ROS) and water amount were included to see if there was evidence that the low and high water amount slopes are different. Table shows the estimates (s.e.) and *P*-values for the coefficients from each model.

Direct suppression almost always reduced spread rate to the minimum level that could be estimated by this methodology (as demonstrated in Fig. 5); however, this was not the case for the indirect suppression treatment. This different result is likely due to the difference in effective water depth (per unit treatment area) delivered in each suppression method. Indirect suppression distributed the experimental treatment water volume over approximately twice the area of our direct suppression treatment and therefore the effective water depth delivered by indirect suppression was approximately half that of the direct suppression treatment (e.g. 0.7 mm water depth compared with 1.4 mm water depth for the low water treatment). The two suppression treatments also physically impacted fuel bed structure differently and this may have led to some observed differences. The forceful stream of the direct suppression tactic resulted in fuels in the combustion zone being moved around and broken up, thereby disrupting the ability of the flame front to continue passing through the fuel bed, whereas indirect suppression was applied with a more dispersed stream and did not disrupt the continuity of the fuel bed.

## Duration of suppression-induced fireline hold

### Objective

This analysis was designed to examine the impact of suppression treatments on the duration of fireline holding time by using time series data and examining the period immediately before suppression with the length of time required for a fire to resume active spread.

### Analysis

The duration of suppression-induced fireline holding time was determined by examining the length of time, in seconds, for which the rate of spread was reduced and showed less variability after suppression. Typically, the post-suppression spread rate was reduced close to 0 m/s and these spread rate observations exhibited virtually no variability. The resumption of more vigorous flaming spread was indicated by not only an increase in rate of spread, but also an obvious increase in variability of the spread rate observations in the IR-based time series. In cases where the rate of spread did not decrease after suppression, the duration of hold was determined to be zero.

A four-way factorial ANOVA comparison of suppression hold time in seconds for each of the four treatment factors was made to assess whether there was evidence of an influence of the four treatment factors on duration of suppression-induced hold. When treatment groups or interactions between treatments showed strong evidence of a difference between groups ($P < 0.05$), Tukey's Honest Significant Difference post-hoc tests were performed to determine which specific treatment group means were different and the direction of this difference.

### Findings

On average, suppression held the fireline for 2 min (average 123 s; s.d. 17 s). In the cases where suppression eliminated the re-establishment of sustainable flaming spread ($n = 17$), the duration of the suppression-induced hold was set equal to infinity. There were also nine cases where the suppression-induced hold was 0 s. The amount of water was the only treatment factor that exhibited some evidence of a main effect ($F = 6.43$, $P = 0.1$), with interactions ($P < 0.05$) between suppression type and water amount, suppression type and fuel type, and suppression type, water amount and fuel type. Tukey's post hoc test revealed strong evidence that the high water treatment resulted in a greater duration of hold, with an average hold time 64 s longer ($P < 0.05$) than the low water treatment condition. This interaction between suppression type and water amount was further examined, showing very strong evidence of a difference for indirect suppression and water amount; the high water treatment resulted in a 120-s increase in duration of hold compared with low water for indirect suppression only ($P < 0.01$). This finding is likely due to the increased fuel moisture content as a result of the high water condition. This increase in fireline holding time as a function of the water treatment amount was not observed for the direct suppression treatments, likely because the water was being applied directly into the combustion zone, and any impact of the effects of the greater water amount used here might be hidden by the reheating possible from the remaining active combustion zone.

The comparison between average fire behaviour before suppression and the resulting duration of suppression-induced hold was then examined to see if spread rate and intensity influenced fireline hold time. In general, as expected, as the average rate of spread (Fig. 6) or fireline intensity before suppression increased, the ability of

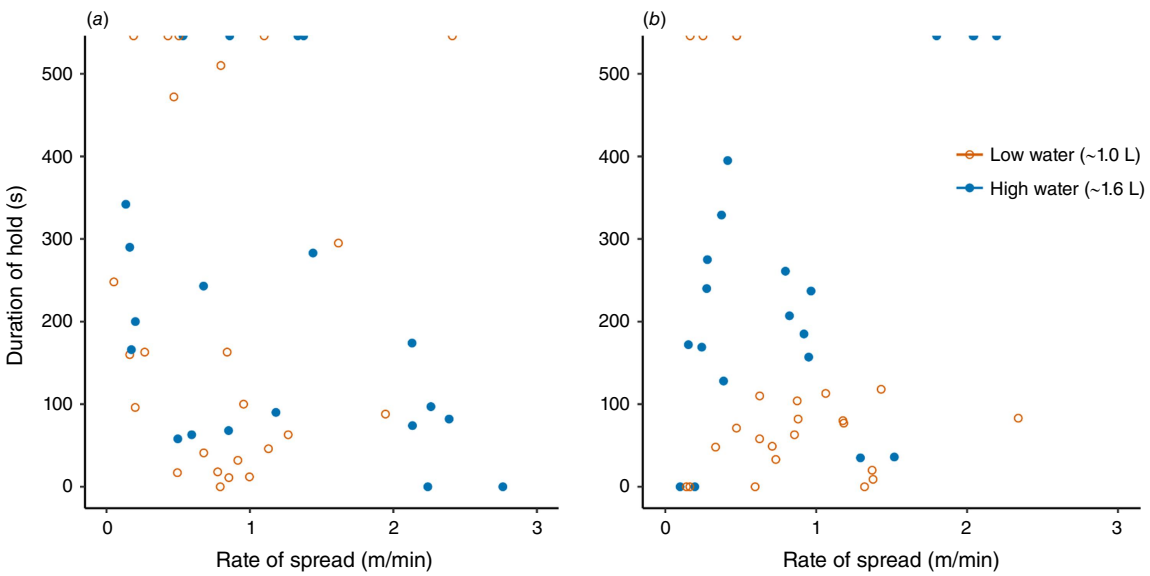


**Fig. 6.** Relationship between the average fire behaviour before suppression and the duration of suppression-inducted fireline hold: (*a*) the average rate of spread before suppression and the duration of suppression-induced hold for direct suppression; (*b*) the average rate of spread before suppression and the duration of suppression-induced hold for indirect suppression. The points at the top represent observations with a duration of hold set to infinity.

suppression to hold the fireline decreased. The interaction of suppression type and water amount is evident for indirect suppression, with low and high water treatments showing separation in the hold durations in both rate of spread (Fig. 6) and fireline intensity plots (Supplementary Appendix S3).

## Influence of suppression on fire radiative energy release

### Objective

This analysis was designed to examine the impact of water application on the energy released from a fire, as measured by a decrease in FRED.

### Analysis

For the analysis of FRED, the entire burn pad, as opposed to isolating the inner 2.44 m, was used to account for fuel consumption across the entire fuel bed. First, the pixels on the burn pad that received suppression treatment were extracted by isolating the pixels that had fire arrival times between the suppression start and end times. Consequently, for each burn, each pixel in the fuel bed was classified as being one of three types; pixels that had (1) no suppression, (2) direct suppression, or (3) indirect suppression. FRED values were summarised for each of these groupings. The mean FRED values for each of these groups for each burn were compared using visualisations of the distributions and one-way ANOVA comparisons of the means to determine if water did affect the total energy released from the fire, and to estimate the strength of evidence of any difference between direct versus indirect suppression. Interactions between water amount, fuel type and fuel load were examined for each of the suppression categories.

Because FRED integrates radiative energy released over the full duration of the burn, which includes both the flaming and extended period of smouldering combustion, the smouldering or glowing combustion contributed to this total energy release. The energy from this extended period of fuel burn-out could mask any signal of suppression being applied to influence flaming combustion. We therefore examined an energy release measure that represents energy released during only the flaming portion of the fire, which we refer to as 'flaming FRED' (F-FRED). This metric integrates radiative energy measured from each pixel starting when the FRPD at that pixel exceeds a value of 0, indicating the cell is now likely flaming, for a pre-defined period of time. Flaming combustion times of 45 s (slightly longer than the time observed by Kidnie and Wotton (2015) for grass fuels, and 60 s (consistent with Taylor *et al.* 2004) for pine fuels were used.

### Findings

In the no-suppression areas, the low fuel load pine fuel group (1.0 kg/m$^2$) had an average FRED of ~1700 kJ/m$^2$ (s.d. 295), the high fuel load pine fuel group (1.5 kg/m$^2$) had an average FRED of ~3000 kJ/m$^2$ (s.d. 123), and the grass fuel group (1.0 kg/m$^2$) had an average FRED of ~1700 kJ/m$^2$ (s.d. 113). Although a reduction in FRED was anticipated in cells that received suppression treatment, statistical evidence supporting this was not strong ($F = 2.29$, $P = 0.1$), with FRED reductions of 246 kJ/m$^2$ for direct suppression and 117 kJ/m$^2$ for indirect suppression. The primary factor contributing to differences in FRED was fuel load ($F = 86.35$, $P < 0.001$). On average, the high fuel load released nearly 80% (1265 kJ/m$^2$) more energy than the low fuel load. Assuming both fuel loadings burned with identical consumption efficiency, we would expect to observe an ~50% greater energy release from the higher fuel loading.

The absence of clear differences in energy release between treated and untreated cells is likely due to FRED integrating energy release throughout the burn, including the smouldering combustion phase. An analysis of F-FRED (which focuses specifically on the flaming combustion phase) indicated that F-FRED represents ~50% of the total radiative energy of FRED (Fig. 7*a*). This proportion remained consistent across various cells on the burn pad (Fig. 7*a*). Examples of a typical FRPD time series observed from untreated (Fig. 7*b*) and treated cells (Fig. 7*c*, *d*) show a clear decrease in FRPD with suppression.

Comparisons between untreated areas of the burn pad and cells that received suppression demonstrated strong evidence that the cells that received suppression had less radiative energy release, as demonstrated by reductions in F-FRED, than the untreated areas ($F = 10.91$, $P < 0.001$). Direct suppression resulted in an average reduction of 258 kJ/m$^2$, and indirect suppression led to a reduction of 189 kJ/m$^2$ compared with energy observed from the untreated portions of the fuel bed. However, there is no evidence that suggests there was a difference in flaming energy between the suppression treatment types ($P = 0.45$), or the amount of water delivered to the treatment areas ($F = 2.16$, $P = 0.15$). The high fuel load grouping had a 34% higher F-FRED, a difference of 233 kJ/m$^2$ compared with low fuel load experiments, below the expected 50% increase due to increased fuel loading.

Water inhibits the heating of forest fuels to combustion temperature by absorbing energy from the combustion reaction to heat and vaporise it. That energy, ~2600 kJ/kg at 100°C, accounts for the latent heat of vaporisation of water and the energy required to heat the water in the suppression zone from ambient (assumed to be ~20°C) up to 100°C. If we assume the entire mass of water added to the fuel during suppression acts as an energy sink during combustion, the reduction in net energy release expected compared with untreated portions of the fuel bed can be estimated. Once scaled down by the radiative fraction of 0.15 (Johnston *et al.* 2017), the impact of 1 L of water in the combustion zone on the observed radiative energy is ~390 kJ/m$^2$. When accounting for the water coverage area

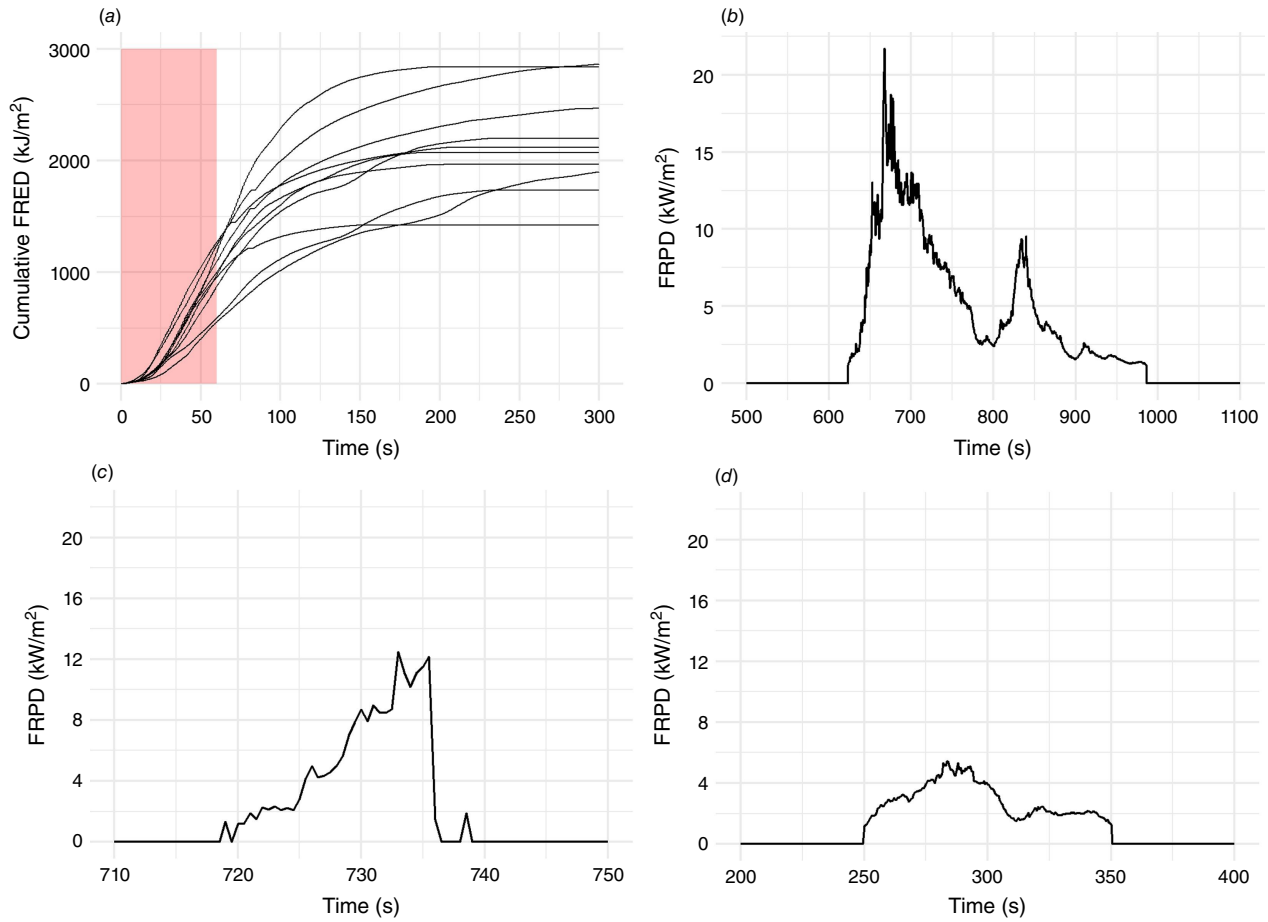


**Fig. 7.** (*a*) Cumulative FRED i(kW/m$^2$) through time for a sub-sample ($n$ = 10) of pixels in a burn that did not receive suppression. The red shaded area highlights the first 60 s after the pixel was ignited (i.e.. FRP > 0). (*b*) Time series of FRPD (kW/m$^2$) for a single pixel that did not receive suppression. (*c*) Time series for FRPD (kW/m$^2$) for a single pixel that received direct suppression. (*d*) Time series for FRPD (kW/m$^2$) for a single pixel that received indirect suppression. All figures are from B1.

of the suppression treatments, this results in a theoretical energy reduction of 550 kJ/m$^2$ for the low water and 900 kJ/m$^2$ for the high water direct suppression treatments (Fig. 8*a*), and 270 kJ/m$^2$ for the low water and 430 kJ/m$^2$ for the high water indirect suppression treatments (Fig. 8*b*). These observed values are lower than the theoretically expected energy loss (Fig. 8), although the reduction in F-FRED alone suggests the IR imagery captures the physical effects of water application in a flaming combustion zone.

The comparison of reductions in radiative energy release measured by F-FRED revealed that suppression areas had 30% less energy measured compared with unsuppressed areas, whereas the same comparison with FRED only showed a ~15% reduction in measured energy. Although the energy measured from F-FRED in the suppression areas is slightly lower than we would expect given the heat of vaporisation of water (Fig. 8), this outcome is not surprising because there is a possibility of water loss in both suppression treatments. The direct suppression stream likely penetrates through the fuel complex to the surface of the Marinite boards, which would reduce the ability of the water to inhibit combustion energy release. Similarly, for the indirect suppression treatment, it is likely that some of the water sprayed onto the fuel bed evaporated as the flame front advanced towards the suppression area.

## Discussion and considerations for future experiments

This experiment was a preliminary investigation of the use of IR imagery to quantify fire suppression effectiveness by examining its direct impact on fire behaviour (i.e. reduction in fire spread rate and duration of holding time), and also by specifically estimating the reduction in the energy released from a flaming fire front due to water application. Using fine temporal and spatial scale IR imagery methods, we observed changes in fire behaviour due to suppression and quantified the duration of the reduction (i.e. holding time). Additionally, we detected the suppression signal on energy

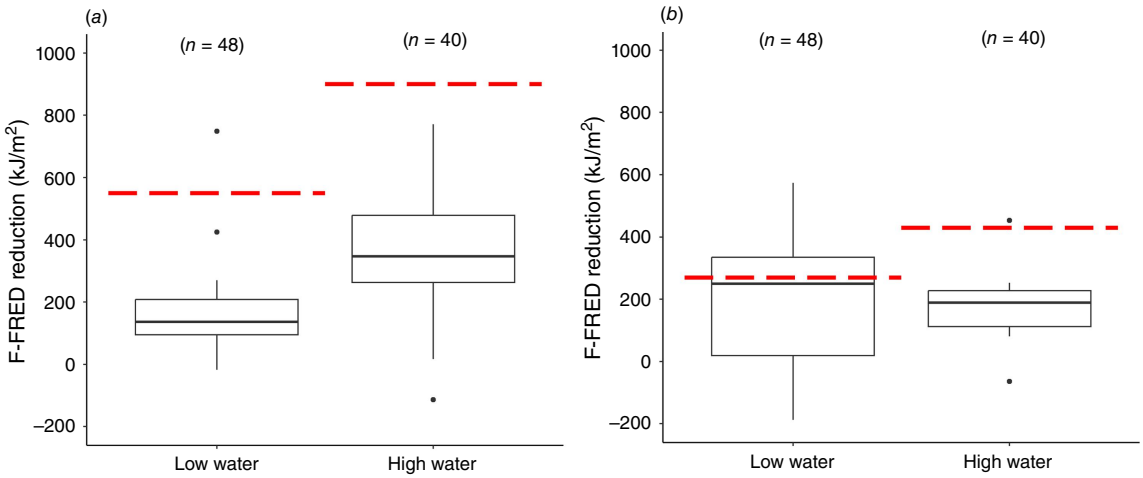


**Fig. 8.** Boxplots of the observed values for the reduction in F-FRED for (*a*) direct suppression, and (*b*) indirect suppression compared with the untreated cells. The red dashed lines represent the theoretical energy reduction given the amount of water added in the treatment area. For direct suppression, the low water condition has a theoretical energy reduction of 550 kJ/m$^2$ and the high water has a reduction of 900 kJ/m$^2$. For indirect suppression, the low water condition has a theoretical energy reduction of 270 kJ/m$^2$ and the high water has a reduction of 430 kJ/m$^2$.

release through an analysis of radiative energy during the flaming combustion phase (i.e. F-FRED).

The site where these experimental burns were conducted was designed specifically to assess the capabilities of IR technology to measure fire behaviour, rather than to conduct controlled experiments that isolate specific fire behaviour attributes (e.g. controlling wind speed to control for fire spread and fireline intensity) as was the case in previous studies (Plucinski *et al.* 2017; Plucinski and Sullivan 2024). Our goal was to explore the ability of this IR technology to measure the influence of suppression on fire behaviour, which did not necessarily require a strictly controlled environment. However, in retrospect, we recommend that future studies be carried out under more controlled experimental conditions. Future experiments should consider increasing power by using just one fuel type, or using more replicates of each fuel type, to ensure a larger sample of burns in each treatment category. To estimate the variability in the amount of suppression effort applied between treatments, the suppression system (e.g. soft backpack pump) should be weighed before and after suppression to precisely quantify the amount of water applied to the treatment area.

The absence of a clear signal regarding the impact of water amount and coverage level on fire behaviour is likely due to environmental variability, particularly the high fluctuations of wind velocity thatled to temporal variation in fire behaviour during each burn. Hourly wind speed estimates from a nearby weather station (~100 m from the burn site at an anemometer height of 10 m) were used, but having fine-scale (i.e. seconds) wind observations at ~1.5-m height directly at the site would provide insight into the fine temporal scale dynamics of fire behaviour observed, distinguishing between suppression and wind effects.

We recognise that the water amounts chosen for this experiment may be less than what might be delivered in practice. We chose a water delivery method and volume that would yield varying effects on fire behaviour with the anticipated fire intensities according to the fuel loads used, as reported by Johnston *et al.* (2017). However, we note that the water amounts applied in the present study, ranging from 0.7 to 2.3 mm of rainfall equivalent, align closely with coverage levels observed from a single drop of commonly used airtankers in the boreal forest. For example, the Canadair CL-415 skimmer airtanker – a widely used airtanker across the globe – delivers most (75%) of its drop footprint with a coverage level of less than 2.5 mm (McFayden *et al.* 2023*b*). This demonstrates that our suppression treatment amounts are comparable, at least in terms of coverage levels, with operational aerial suppression practices. Future studies should adapt the methods to more accurately measure the area over which the water was applied and to relate suppression treatment levels directly to coverage levels in terms of rainfall equivalent (e.g. 0.5 mm or greater). Doing so would enable a more consistent comparison of suppression treatment methods and align more closely with the concept of coverage level commonly used in studies of aerial suppression effectiveness. Such refinements would allow researchers to better connect experimental findings with real-world suppression practices and could help validate and provide quantitative evidence for already developed suppression models (Stechishen and Little 1971; Loane and Gould 1986; McFayden *et al.* 2023*b*).

Safety concerns and fuel bed characteristics precluded our ability to ignite higher-intensity fires to investigate the impact of suppression effort on fires of greater intensities (i.e. fireline intensity >500 kW/m). For the lower-intensity

fires we ignited (<500 kW/m), we found that suppression coverage amounts of 1.0 mm and greater reduced the rate of spread to the minimum observable level. Despite this limitation, the finding that IR technology captures the impact of suppression on energy release is a significant contribution for future research considerations. Fireline intensity, and therefore the amount of energy release from the fire, is an important fire behaviour attribute often used to assess suppression resource use thresholds and the extent to which ground suppression crews can safely work on the fireline (Hirsch and Martell 1996; Taylor and Alexander 2018). Airborne IR platforms offer an advantage for studying suppression effectiveness in actual wildfire settings and on fires with higher intensity. Unlike ground-based methods, which often require pre- and post-fire access, airborne IR can be used to measure fire behaviour attributes and suppression impacts at fine spatial and temporal scales without the need for ground sampling. These platforms can also be deployed in real time during suppression operations, capturing thermal imagery that can be used to determine fireline intensity, rate of spread and other metrics immediately before, during and after suppression efforts. Such research is under way; Wheatley *et al.* (2024) describe ongoing research using an airborne IR platform to observe airtanker suppression action on actual wildfires where they quantify the reduction in fireline intensity and assess the duration of suppression effects under operational conditions. By using airborne IR imagery, researchers are able to evaluate the immediate and lasting effects of suppression on fire behaviour, providing critical insights into the effectiveness of various suppression resources.

## Supplementary material

Supplementary material is available online.

## References


Àgueda A, Pastor E, Planas E (2008) Different scales for studying the effectiveness of long-term forest fire retardants. *Progress in Energy and Combustion Science* **34**, 782–796. doi:10.1016/j.pecs.2008.06.001

Blakely AD (1985) Combustion recovery: a measurement of fire retardant extinguishment capability. USDA Forest Service No. INT-352. (Intermountain Forest and Range Experiment Station: Odgen, Utah)

Blakely AD (1990) Combustion recovery of flaming pine needle fuel beds sprayed with water/MAP mixtures. USDA Forest Service No. INT-421. (Intermountain Forest and Range Experiment Station: Odgen, Utah)

Budd GM, Brotherhood JR, Hendrie AL, Jeffery SE, Beasley FA, Costin BP, Zhien W, Baker M M, Cheney NP, Dawson MP (1997) Project Aquarius 4. Experimental bushfires, suppression procedures, and measurements. *International Journal of Wildland Fire* **7**(2), 99–104. doi:10.1071/WF9970099

Byram GM (1959) Combustion of forest fuels. In 'Forest fire: control and use'. (Ed. KP Davis) pp. 61–89. (McGraw-Hill: New York, NY, USA)

Canadian Interagency Forest Fire Centre (CIFFC) (2021) Canada Report 2021. Retrieved from https://www.ciffc.ca/sites/default/files/2022-02/Canada_Report_2021_Final.pdf [verified 29 June 2024]

CIFFC (2023) Canadian Wildland Fire Glossary. Retrieved from https://www.ciffc.ca/publications/glossary [verified 29 June 2024]

George CW (1985) An operational retardant effectiveness study. *Fire Management Notes* **46**(2), 18–23.

George CW (1988) An update on the Operational Retardant Effectiveness (ORE) program. In 'The Art and Science of Fire Management. Proceedings of the First Interior West Fire Council Annual Meeting and Workshop'. Information report NOR-X-309. pp. 24–27. (Forestry Canada, Northern Forestry Centre)

Gibos K, Ault R (2007) Exploring a method to evaluate the ability of water enhancing gel to stop wildfire spread. Report. (FPInnovations Wildfire Operations Research; Hinton, Alberta) Available at https://library.fpinnovations.ca/en/permalink/fpipub9381 [verified 29 June 2024]

Giménez A, Pastor E, Zárate L, Planas E, Arnaldos J (2004) Long-term forest fire retardants: a review of quality, effectiveness, application and environmental considerations. *International Journal of Wildland Fire* **13**, 1–15. doi: 10.1071/WF03001

Hansen R (2012) Estimating the amount of water required to extinguish wildfires under different conditions and in various fuel types. *International Journal of Wildland Fire* **21**, 525–536. doi:10.1071/WF11022

Hirsch KG, Martell DL (1996) A review of initial attack fire crew productivity and effectiveness. *International Journal of Wildland Fire* **6**(4), 199–215. doi:10.1071/WF9960199

Johnston J, Wheatley M, Wooster M, Paugam R, Davies G, DeBoer K (2018) Flame-front rate of spread estimates for moderate scale experimental fires are strongly influenced by measurement approach. *Fire* **1**(1), 16. doi:10.3390/fire1010016

Johnston JM, Wooster MJ, Paugam R, Wang X, Lynham TJ, Johnston LM (2017) Direct estimation of Byram's fire intensity from infrared remote sensing imagery. *International Journal of Wildland Fire* **26**(8), 668–684. doi:10.1071/WF16178

Johnston JM, Jackson N, McFayden C, Ngo Phong L, Lawrence B, Davignon D, Wooster MJ, van Mierlo H, Thompson DK, Cantin AS, Johnston D, Johnston LM, Sloane M, Ramos R, Lynham TJ (2020) Development of the user requirements for the Canadian WildFireSat Satellite Mission. *Sensors* **20**(18), 5081. doi:10.3390/s20185081

Kidnie S, Wotton BM (2015) Characterisation of the fuel and fire environment in southern Ontario's tallgrass prairie. *International Journal of Wildland Fire* **24**(8), 1118–1128. doi:10.1071/WF14214

Loane IT, Gould JS (1986) 'Aerial suppression of bushfires: cost–benefit study for Victoria.' (National Bushfire Research Unit, CSIRO Division of Forest Research)

McFayden C, Hope E, Johnston JM, Cantin A, Crowley MA, de Jong M, Thompson DK, Young D (2023*a*) WildFireSat pathway for implementation and uptake in provincial and territorial fire management agencies. Information Report GLC-X-36. 45 p. (Great Lakes Forestry Centre, Canadian Forest Service)

McFayden CB, Wotton BM, Robinson JW, Johnston JM, Cantin A, Jurko NM, Boucher J, Wheatley M, Ansell M, Boychuk D, Russo B (2023*b*) Reference guide to the drop effectiveness of skimmer and rotary wing airtankers. Information Report GLC-X-35. (Canadian Forest Service, Great Lakes Forestry Centre) Available at https://cfs.nrcan.gc.ca/publications?id=41009 [verified 28 June 2024]

Merrill DF, Alexander ME (1987) 'Glossary of forest fire management terms.' (Canadian Committee on Forest Fire Management, National Research Council of Canada: Ottawa, ON, Canada)

Pastor E, Àgueda A, Andrade-Cetto J, Muñoz M, Pérez Y, Planas E (2006) Computing the rate of spread of linear flame fronts by thermal image processing. *Fire Safety Journal* **41**(8), 569–579. doi:10.1016/j.firesaf.2006.05.009

Paugam R, Wooster MJ, Roberts G (2012) Use of handheld thermal imager data for airborne mapping of fire radiative power and energy and flame front rate of spread. *IEEE Transactions on Geoscience and Remote Sensing* **51**(6), 3385–3399. doi:10.1109/TGRS.2012.2220368

Penney G, Habibi D, Cattani M, Carter M (2019) Calculation of critical water flow rates for wildfire suppression. *Fire* **2**(1), 3. doi:10.3390/fire2010003

Pérez Y, Pastor E, Planas E, Plucinski M, Gould J (2011) Computing forest fires aerial suppression effectiveness by IR monitoring. *Fire Safety Journal* **46**(1–2), 2–8. doi:10.1016/j.firesaf.2010.06.004

Plucinski MP (2019*a*) Fighting flames and forging firelines: wildfire suppression effectiveness at the fire edge. *Current Forestry Reports* **5**, 1–19. doi:10.1007/s40725-019-00084-5

Plucinski MP (2019*b*) Contain and control: wildfire suppression effectiveness at incidents and across landscapes. *Current Forestry Reports* **5**, 20–40. doi:10.1007/s40725-019-00085-4

Plucinski MP, Pastor E (2013) Criteria and methodology for evaluating aerial wildfire suppression. *International Journal of Wildland Fire* **22**(8), 1144–1154. doi:10.1071/WF13040

Plucinski MP, Sullivan AL (2024) Methodologies for quantitatively comparing the effectiveness of chemical retardants for direct and indirect wildfire suppression using a combustion wind tunnel. *Fire Safety Journal* **143**, 104056. doi:10.1016/j.firesaf.2023.104056

Plucinski MP, Sullivan AL, Hurley RJ (2017) A methodology for comparing the relative effectiveness of suppressant enhancers designed for the direct attack of wildfires. *Fire Safety Journal* **87**, 71–79. doi:10.1016/j.firesaf.2016.12.005

Stechishen E (1970) Measurement of the effectiveness of water as a fire suppressant. Information Report FF-X-23. pp. 12–14. (Forest Fire Research Institute: Ottawa, Canada)

Stechishen E, Little EC (1971) 'Water application depths required for extinguishment of low intensity fires in forest fuels.' (Forest Fire Research Institute, Department of Fisheries and Forestry)

Stocks BJ, Martell DL (2016) Forest fire management expenditures in Canada: 1970-2013. *Forestry Chronicle* **92**(3), 298–306. doi:10.5558/tfc2016-056

Taylor SW, Alexander MW (2018) 'Field guide to the Canadian Forest Fire Behaviour Prediction (FBP) system.' (Northern Forestry Centre, Canadian Forest Service)

Taylor SW, Wotton BM, Alexander ME, Dalrymple GN (2004) Variation in wind and crown fire behaviour in a northern jack pine–black spruce forest. *Canadian Journal of Forest Research* **34**(8), 1561–1576. doi:10.1139/x04-116

Van Wagner CE, Taylor SW (2022) Theoretical amounts of water to put out forest fires. Information Report BC-X-458. (Canadian Forest Service, Pacific Forestry Centre) Available at https://www.researchgate.net/profile/Sw-Taylor/publication/363854973_Theoretical_Amounts_of_Water_to_Put_Out_Forest_Fires/links/6331f3c66063772afd94a548/Theoretical-Amounts-of-Water-to-Put-Out-Forest-Fires.pdf

Wheatley M, Ifimov G, de Jong M, Naprstek T, Wotton M, Reid R, McFayden C, Leblanc G, Johnston J, Robinson J (2024) 'How effective is aerial suppression? We need to find out.' (Canadian Wildland Fire & Smoke Newsletter, Canada Wildfire) Available at https://www.canadawildfire.org/_files/ugd/90df79_7e49f7f96579418e960154fe60c6bc19.pdf

Wooster MJ, Zhukov B, Oertel D (2003) Fire radiative energy for quantitative study of biomass burning: derivation from the BIRDs experimental satellite and comparison to MODIS fire products. *Remote Sensing of Environment* **86**(1), 83–107. doi:10.1016/S0034-4257(03)00070-1

Wooster MJ, Roberts G, Perry GLW, Kaufman YJ (2005) Retrieval of biomass combustion rates and totals from fire radiative power observations: FRP derivation and calibration relationships between biomass consumption and fire radiative energy release. *Journal of Geophysical Research: Atmospheres* **110**(D24), D21111. doi:10.1029/2005JD006018

**Data availability.** The authors do not have permission to share the data.

**Conflicts of interest.** David Martell is an Associate Editor of International Journal of Wildland Fire. To mitigate this potential conflict of interest he did not have editor-level access to this paper during the peer review. Authors have no other conflicts of interest to declare.

**Declaration of funding.** We acknowledge the support of the Natural Science and Engineering Research Council of Canada (NSERC) through a Canada Graduate Scholarship – Doctoral to MW and through its Discovery Grant Program (RGPIN-2021-03920) to DGW.

**Acknowledgements.** We greatly acknowledge the staff at the Canadian Forest Service (CFS) Great Lakes Forestry Centre for their assistance in executing the experimental burns. We also thank Matthew Ansell (CFS) for their assistance in data processing, and Matt Plucinski (CSIRO) for his comments on this manuscript.

**Author affiliations**

[A]Institute of Forestry and Conservation, John H. Daniels Faculty of Architecture, Landscape and Design, University of Toronto, Toronto, ON M5S 3B3, Canada.

[B]Great Lakes Forestry Centre, Canadian Forest Service, Natural Resources Canada, Sault Ste Marie, ON P6A 2E5, Canada.

[C]Department of Statistical and Actuarial Sciences, University of Western Ontario, London, ON N6A 5B7, Canada.